The role of CO on microexplosion of iron particle in methane-air premixed flames

Aris Purwanto, Bo-Cheng Zhuang, Yueh-Heng Li
Department of Aeronautics and Astronautics, National Cheng Kung University, Taiwan

Abstract

When aluminum is mixed with zirconium, aluminum would evaporate and oxidize with oxygen. Alumina would attach with zirconium. Nitrogen and oxygen would dissolve into zirconium particles and form bubbles. Then, bubbles would grow gradually due to nucleation. However, the severe growth rate of bubbles led to micro-explosion phenomena. It is a so-called particle microexplosion for Al-Zr hybrid metal combustion. In the previous study, an iron-coal mixture was delivered to methane-air premixed flames, and an exciting particle microexplosion phenomenon was observed during this experiment. In our proposed speculation, the presence of CO may dissolve in iron particles and produce bubbles. A portion of CO bubbles may react with iron and yield iron carbonyl ($Fe(CO)_5$).Consequently, the merged bubbles would gradually increase their inner pressure, and meantime combustible mixture of iron carbonyl and oxygen may induce the microexplosion. To elucidate the role of CO in the microexplosion mechanism, a hybrid iron-methane air premixed flame diluted with different concentrations of CO was used to observe the mechanism of particle microexplosion. The particle concentration varied from 0 – 350 g/m^3. Therefore, it conjectures that CO was dissolved into iron particles, giving rise to expanding the volume of a metal particle and inducing microexplosion.

Keywords: hybrid flame, iron combustion, microexplosion, iron carbonyl

1. Introduction

Metal particles, for instance, aluminum, iron, magnesium, and zirconium, are the most abundant resource on the earth. Due to the higher energy density and high chemical reaction to enhance combustion stability, metal as a rocket propellant has been used for a long year [1-3]. A two-phase hybrid combustible mixture of solid and gaseous fuel has been used in many practical applications, such as coal combustion and synthesis. A simple system to study multi-front phenomena which consist of two mixture fuel that have very different activation energy and reaction mechanism these phenomena has been studied theoretically by Goroshin *et al.* [4] and experimentally for CH_4-NO_2-O_2 mixture [5] and hybrid aluminum-methane flame [6]. Bergthorson [7] proposed a concept of recyclable metal fuel for clean and zero-carbon power.

In general, metal particle combustion could be divided into three different combustion modes based on the characteristic of metal and oxidation reaction of metal in hydrocarbon fuel [7, 8]. These modes not only affected reaction type but also affected the particle size of the combustion product. Modes A can be categorized as vapor phase combustion, which means particles may become metal vapor, and that metal vapor reacts with an oxidizer to release heat. In the hydrocarbon flame, micro diffusion flame appears in the metal vapor region. This mode can be categories as homogenous combustion. Modes B is heterogeneous combustion but forming a gaseous and sub-oxide. The gaseous could react with an oxidizer, but a micro diffusion flame appears at the surface of metal particles. The interesting modes are Modes C The interesting combustion phenomenon that occurred in mode C may react heterogeneously and produce metal oxides equivalently,

which are easier to be captured due to the aggregation of produced porous solid metal oxides. In metal combustion, a minimum concentration of metal particles is essential for heat release to support metal flame propagation. It also depends on the availability of oxygen and the chemical reaction rate between metal as fuel and oxidizer. Moreover, the size of a solid combustion product can be linked to the combustion modes to which fuel belongs.

Regarding the combustion behaviors of metal, a particle is a particle microexplosion. Microexplosion has been studied on single-particle combustion of Al-Mg [9], Al-Zr wire alloy combustion [10], and combustion of a pure metal particle of Ti and Zr [11, 12]. Wainwright *et al.* [13] used X-Ray phase contrast imaging and a high-speed camera to observe internal bubbling and particle microexplosion of ball mixed Al: Zr particle in the wire combustion under various conditions. They proposed a mechanism of Al: Zr particle microexplosion when the Al particle heated and became an aluminum vapor heated the particle while N_2 dissolved into the particle and then generated Al-Zr-N alloy containing some oxygen. During these phenomena, the researcher concluded that the rapid bubbling triggered microexplosion and the slow bubbling in the particle would result in spherical metal particles.

The aim of this study is to underlying the micro-explosion phenomena of iron hybrid combustion. In our previous study [14], we mixed iron particles with aluminum and coal particle. We want to examine combustion interaction between two particles with different combustion modes. Within this experiment, we found exciting metal combustion phenomena, a particle microexplosion in the Fe-Coal case. According to the experiment result, we concluded that the micro explosion phenomena come from a high concentration, CO gas coming from coal combustion product. CO may have diffused through the surface of the iron particle, and CO reacted with iron to form explosive gas $Fe(CO)_5$. In this experiment, we dilute CO gas concentration in methane-air premixed flame to understand the role of CO gas on micro-explosion.

2. Experimental Methods

2.1. Material Preparation

Particle size is a crucial parameter of solid fuel combustion, Bergthorson [8] specified that iron particle sizes 20 μm of iron have similar burning velocities with gaseous combustion. In this experiment, we used 2.548 μm particles, particle shape and surface characteristics were examined by scanning electron microscopy (SEM) Energy-dispersive X-ray spectroscopy (EDS) (SEM-EDS: Hitachi 4800, Japan). Sinchuan Zichuan New Material Technology Co. Ltd. (Chengdu, Sichuan, China) provided the iron particle sample. **Table 1** present the information on particle morphology and chemical composition of the iron particle.

Table 1 Chemical composition of iron particle

Material	Category	Shape	Composition	
			Chemical Composition	Concentration (%)
Iron	Fine Powder	Irregular cluster	Fe	98.86
			Mn	0.30
			P	0.03
			S	0.01
			C	0.01
			Si	0.02

2.2. Burner and feeding system

The coaxial stainless-steel burner is used in **Figure 1**(a) with an inner diameter of 11.5 mm and an outer diameter of 14mm, and the overall length is 120mm. The design of the inner tube nozzle is a concentric reduction. This design can help to laminarize the mixture before exiting from the nozzle. This burner has been used in our previous experiment [14]. The feeding system of this experiment was a low concentration particle disperser (RBG 1000 Palas GmbH, Germany), as shown in **Figure 1**(b). The principle of this system is based on the rotating brush generator, which disperses dry, non-cohesive particles into an airborne, A pivoted brush with a cylindrical tube located inside the dispersion head. The piston pushes the particle inside the dispersion head with a constant speed set using an electronic panel, and a rotating brush disperses the powder into the outlet port of the particle dispersion system.

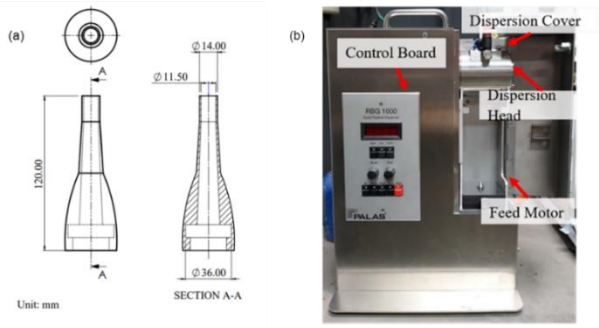

Figure 1 (a) Coaxial stainless-steel burner, (b) photograph of an aerosol generator

2.3. Experimental Apparatus

Figure 2 show the experimental apparatus of combustion of CH4-CO-Air premixed flame, the particle dispersion was used to disperse particle into the nozzle, and the feeding rate was controlled by electronics panel, the carrier gas was mixed with the metal particle in advance. It is delivered into the T-junction for mixing with CH_4-CO before exiting the combustion nozzle. In all cases, the overall equivalent ratio was fixed in stoichiometric value. The Copper-plate captured the combustion product with a purity of 99%. The copper plate was attached in stainless steel reverse tweezer (P-651, Hozan, Japan) with a tip of 0.20mm and double action actuator. A Microcontroller board (Arduino Mega 2650) was used to manage the actuator's timing to remain within the flame for 1.5 s.

The combustion behavior of hybrid flame was observed by a photograph that was captured using a Single Lens Reflex Camera (SLR) camera (D80, Nikon, Japan) attached to a large aperture lens (30mm: F1.4 EX DC HSM, Sigma, USA). The camera was set in (ISO 100, Shutter speed 1/20s, F 10). The particle microexplosion was monitored using a high-speed camera (MEMRECAM ACS-2 NAC, Japan) with a macro lens (MACRO 105mm, F2.8 EX DG OS HSM, SIGMA, USA), a frame rate of 30,000 fps and shutter speed of 38.5 μs was used to determine microexplosion phenomena and burning characteristics of hybrid flame.

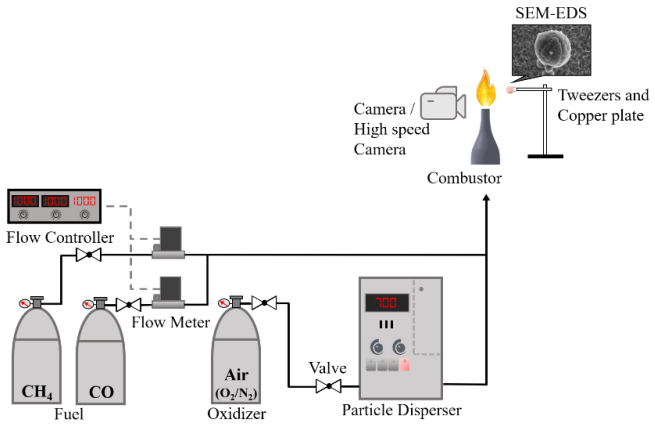

Figure 2 Experimental apparatus and measurement system

3. Result and Discussion

3.1. Metal Combustion

3.1.1. Observation of CH_4-CO-Air premixed flame

A photograph of CH_4-CO-Air is shown in **Figure 3**. The CO concentration was varying from 0% to 10%. The CO concentration has affected the micro explosion phenomena of hybrid iron flames. The outline of the CH_4-CO-Air flame front is presented in **Figure 3**(a); Pure CH_4-Air premixed flame, the blue flame cone was observed on this figure. **Figure 3**(b): is 1% of CO addition the blue flame front also appears on this figure, but some orange flame front didn't appear on this figure compare to **Figure 3**(c) and (d), **Figure 3**(c) is 5% CO addition, blue flame front with orange flame front appear on this figure, the orange flame front is coming from the CO combustion, and **Figure 3**(d) is 10% CO addition.

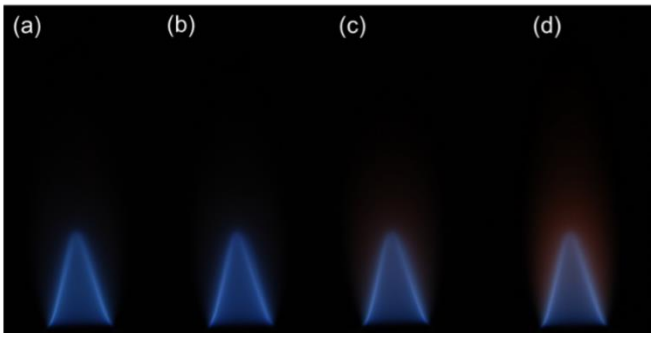

Figure 3 Photograph of CH_4-CO-Air premixed flame with difference CO concentration (a) 0%, (b) 1%, (c) 5%, and (d) 10%.

3.1.2. Observation of Hybrid flame

The effect of various particle feeding rates (126.20, 252.40, 353.35 g/m^3) on hybrid premixed with CO concentration of 0% flame was examined. As shown in **Figure 4**, iron particle was injected into CH_4-CO-Air. **Figure 4**(a) shows the flame image when the feeding rate is set to 0 g/m3, **Figure 4** (b) shows that when the feeding rate was set into 126.20 g/m^{3,} the flame cone of CH4-air flame appears. However, the flame front color become orange. These phenomena happen because the heat release from iron particles was sufficient to form a flame front so that the CH_4-Air flame front can be coupled with an Iron flame front [15]. **Figure 4**(c) and **Figure 4** (d) show that when an iron particle's feeding rate was increased up to 353.35 g/m^{3,} the flame becomes brighter and more stable.

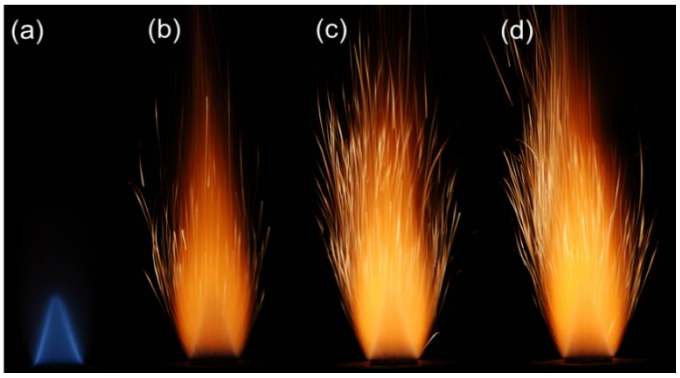

Figure 4 Hybrid Iron-CH4-Air premixed Flame with difference feeding rates (a) 0 g/m^3, (b) 126.20 g/m^3, (c) 252.40 g/m^3, (d) 353.35 g/m^3.

Figure 5 shows the temperature measurement for each particle size. The measurement data start from 0mm above the burner nozzle. The temperature measurement shows that the maximum temperature for all cases is 1500K at the height of 20mm **Figure 5**(a) shows the measurement data for a pure methane-air premixed flame. The maximum temperature for this case was 1500 K at the peak position of the flame front (20mm). **Figure 5** (b) show the measurement data for iron 2-10µm, the data show the temperature distribution of iron 2-10 µm is similar to pure methane-air premixed flames, this data also supported from another research from Julien et al. [15] and Bergthorson [8]. In the study, if an iron particle has size is less than 20µm (<20) would have similar combustion behavior with gaseous flames.

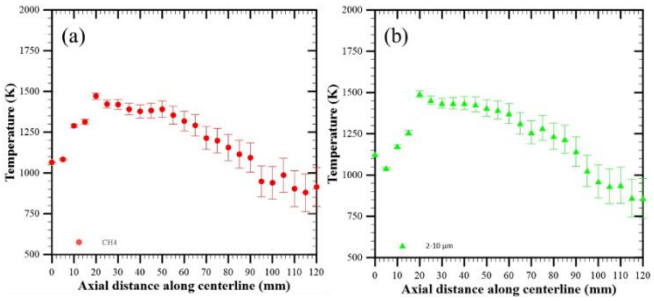

Figure 5 Temperature measurement for CH4-Air and Iron 2-10 µm particles

Figure 6 Shown the hybrid flame of CH_4-CO-Air premixed flame with different CO concentrations with the fixed feeding rate (252.40 g/m^3). **Figure 6**(a) shown the hybrid flame with a 1% CO concentration. During this condition, microexplosion phenomena were observed during this experiment. The flame front of iron and CH_4 become a couple within this condition. **Figure 6** (b) and (c) showed a hybrid flame with 5% and 10% CO concentration respectively, when the CO concentration increased, the probability of microexplosion and the flame is brighter and more stable.

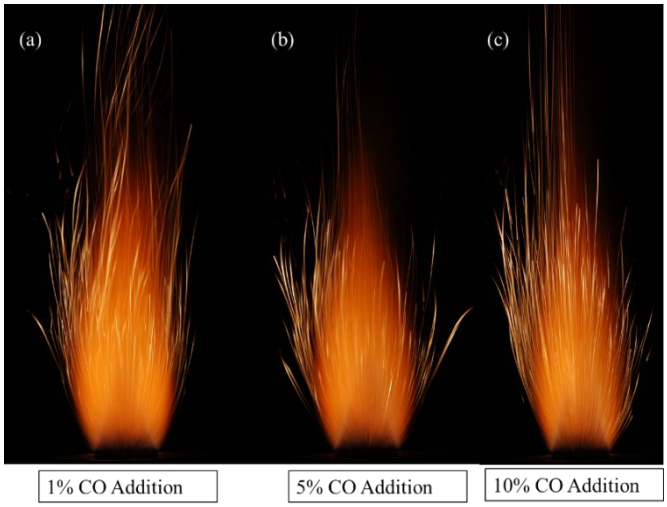

Figure 6 Hybrid Iron-CH4-CO-Air premixed flame with difference CO Concentration (a) 1% CO, (b) 5% CO, and (c) 10% CO

3.2. Combustion Product Analysis

Sampling particles investigated the solid combustion product at three designated positions (DP): within the flame front, 25 mm, and 40 mm heights above the burner. The particles were collected using a grid clipped with a 0.2 mm–tip self-locked tweezer, and their surface geometries and atomic concentrations were analyzed via SEM and EDS. **Figure 7** shown the combustion product. Some particles captured at the flame front featured an irregular shape, whereas others appeared smoother or even spherical because the positions were all located in the upstream region of the reaction zone, and thus, not all the particles had received enough heat to fuse deform. However, once the particles passed through the reaction zone, they were found to be entirely transformed into spherical iron oxides. The combustion product within 25mm has a spherical shape. It seems the iron has reacted with oxygen after heated by the flame front. The combustion product within 40mm has a spherical shape, but the size is smaller than 25mm. It seems that within this zone particle has micro-explosion, and the captured combustion product is coming from the micro-explosion product.

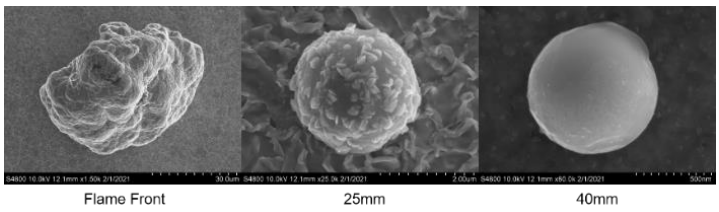

Figure 7 Solid Combustion Product of hybrid flame of Iron-CH4-CO-Air premixed flame

Table 2 shows the EDS result of the surface chemical composition of iron particles at 30mm height above the burner. The result indicates that the iron 2-10 µm contains 36% CO in 10% cases. It is indicated that iron could absorb the CO from the oxidizer and react. This reaction leads to the formation of combustible gas iron carbonyl. The phenomena of microexplosion are elaborated in the next section.

Table 2 Chemical Surface Composition of Iron particles taken from EDS from 25mm height.

CO Concentration	Fe (%)	O (%)	C (%)
0 %	55	21	24
5 %	47	21	32
10 %	43	21	36

3.3. Microexplosion phenomena on hybrid CH4-CO-Air premixed flame

In the hybrid flame of Iron-CH_4-CO-Air premixed flame, particle micro-explosions were induced with the primary, secondary, and tertiary explosions. To analyze the process of the particle microexplosion in hybrid flames, a high-speed camera was engaged to record the behavior of the burning particles in hybrid flames at a fixed particle feeding rate of 252.40 g/m^3 g/m3 (equivalent to 250 mm/h). When the CO concentration was increased, the CO concentration in the post-combustion region would increase drastically. As a result, the CO might diffuse through the Fe particles surface and react with iron to form an explosive gas, iron carbonyl. Furthermore, expanding the gaseous bubble of iron carbonyl inside these particles also increases the surface tensile stress enlargement. Once the tensile stress exceeds the maximum that the oxide-particle surface can withstand, oxide particles would explode. **Figure 8** shown the high-speed camera recorded image of micro-explosion phenomena of Iron-CH4-CO-Air premixed flame with 1% CO concentration.

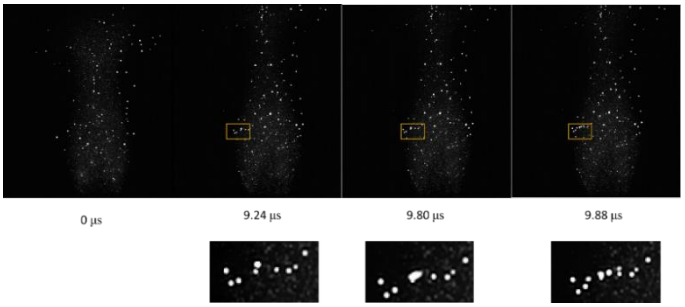

Figure 8 Microexplosion phenomena of Iron-CH_4-CO-Air premixed flame

Figure 9 When the iron particles pass through the reaction zone during the iron combustion stage, the particles burn and oxidized. In these cases, the iron burns in the diffusion regime because the amount of oxygen, in this case, is only 21%. When in the diffusion regime, the oxidizer diffuses into the iron particles and produces iron oxide with a thin shell. Because the amount of oxygen diffuses into the particle is limited, the iron particle becomes an intermediate iron oxide species (FeO). CO reacts with FeO inside the thin shell and becomes an explosive gas bubble, iron carbonyl ($Fe(CO)_5$). The expansion of the gaseous bubble of iron oxide inside the particle also would lead to the enlargement of the surface tensile stress.

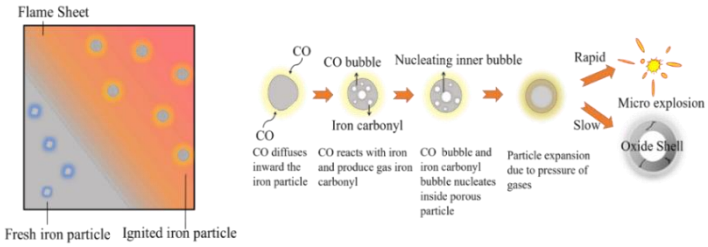

Figure 9 Micro-explosion mechanism of Iron-CH_4-CO-Air premixed flame

4. Conclusions

This present study is to the investigated role of CO on the micro-explosion of a hybrid flame of Iron-CH_4-CO-Air premixed flames. The result shows that particle feeding rates were critical to a coupled flame front of a hybrid flame of Iron-CH_4-CO-Air premixed flame and the particle feeding of 252.40 g/m^3. When the feeding rate was increased, the flame becomes brighter and more stable. Numerous micro-explosions occurred during the Iron-CH_4-CO-Air premixed flames. The phenomenon was hypothesized as the cause of the formation of the iron carbonyl/oxygen coalesced bubbles inside the thin small agglomerate iron oxide shell. The bursting of combustible $Fe(CO)_5/O_2$ bubbles may expand to thin-walled, hollow-shell iron oxide products or fragmentize the iron oxide products.

References

[1] D. S. Sundaram, V. Yang, T. L. Connell, G. A. Risha, and R. A. Yetter, "Flame propagation of nano/micron-sized aluminum particles and ice (ALICE) mixtures," *Proceedings of the Combustion Institute,* vol. 34, pp. 2221-2228, 2013.

[2] T. L. C. Grant A. Risha, Jr., Richard A. Yetter, Vigor Yang, Tyler D. Wood, Mark A. Pfeil, Timothee L. Pourpoin6, Steven F. Son, "Aluminum-Ice (ALICE) Propellants for Hydrogen Generation and Propulsion," presented at the 45th AIAA/ASME/SAE/ASEE Joint Propulsion Conference & Exhibit 2 - 5 August 2009, Denver, Colorado, 2009.

[3] Y. Aly, M. Schoenitz, and E. L. Dreizin, "Ignition and combustion of mechanically alloyed Al–Mg powders with customized particle sizes," *Combustion and Flame,* vol. 160, pp. 835-842, 2013.

[4] M. B. S. Goroshin, And J. H. S. Lee, "Quenching Distance of Laminar Flame in Aluminum Dust Clouds," *Combustion and Flame,* vol. 105, 1996.

[5] M. E. S. M. C. Branch, A. A. Alfarayedhi, and P. J. Van Tiggelen, "Measurements of the Structure of Laminar, Premixed Flames of CH4/NO2/O2 and CH20/NO2/O2 Mixtures," *Combustion and Flame,* vol. 83, 1991.

[6] M. Soo, P. Julien, S. Goroshin, J. M. Bergthorson, and D. L. Frost, "Stabilized flames in hybrid aluminum-methane-air mixtures," *Proceedings of the Combustion Institute,* vol. 34, pp. 2213-2220, 2013.

[7] J. M. Bergthorson, "Recyclable metal fuels for clean and compact zero-carbon power," *Progress in Energy and Combustion Science,* vol. 68, pp. 169-196, 2018.

[8] J. M. Bergthorson, S. Goroshin, M. J. Soo, P. Julien, J. Palecka, D. L. Frost*, et al.*, "Direct combustion of recyclable metal fuels for zero-carbon heat and power," *Applied Energy,* vol. 160, pp. 368-382, 2015.

[9] Y. Feng, L. Ma, Z. Xia, L. Huang, and D. Yang, "Ignition and combustion characteristics of single gas-atomized Al–Mg alloy particles in oxidizing gas flow," *Energy,* vol. 196, p. 117036, 2020.

[10] E. R. Wainwright, T. A. Schmauss, S. Vummidi Lakshman, K. R. Overdeep, and T. P. Weihs, "Observations during Al:Zr composite particle combustion in varied gas environments," *Combustion and Flame,* vol. 196, pp. 487-499, 2018.

[11] J. Yu, X. Zhang, Q. Zhang, L. Wang, K. Ji, L. Peng*, et al.*, "Combustion behaviors and flame microstructures of micro- and nano-titanium dust explosions," *Fuel,* vol. 181, pp. 785-792, 2016.

[12] C. Badiola and E. L. Dreizin, "Combustion of micron-sized particles of titanium and zirconium," *Proceedings of the Combustion Institute,* vol. 34, pp. 2237-2243, 2013.

[13] E. R. Wainwright, S. V. Lakshman, A. F. T. Leong, A. H. Kinsey, J. D. Gibbins, S. Q. Arlington*, et al.*, "Viewing internal bubbling and microexplosions in combusting metal particles via x-ray phase contrast imaging," *Combustion and Flame,* vol. 199, pp. 194-203, 2019.

[14] Yueh-Heng Li, Stalline Pangestu, Aris Purwanto, and Chih-Ting Chen, "Synergetic combustion behavior of aluminum and coal addition in hybrid iron-methane-air premixed flame," *Combustion and Flame,* vol. 228, pp. 364-374, 2021.

[15] P. Julien, S. Whiteley, S. Goroshin, M. J. Soo, D. L. Frost, and J. M. Bergthorson, "Flame structure and particle-combustion regimes in premixed methane–iron–air suspensions," *Proceedings of the Combustion Institute,* vol. 35, pp. 2431-2438, 2015.